Fracture Toughness of 5% Nickel Steel Weldments

Tests demonstrate the suitability of this Armco heat treated steel for cryogenic containment service when properly welded

BY D. A. SARNO, J. P. BRUNER AND G. E. KAMPSCHAEFER

ABSTRACT. A 5% nickel alloy steel* was specifically designed for cryogenic service. The low temperature capability of this steel is attained by composition optimization and microstructural control through a special three-step heat treatment. For particularly critical applications, fracture toughness and fatigue data have been developed. Rotating beam fatigue characteristics, stress intensity (K_c), and fatigue crack growth rate (da/dN vs ΔK) data at cryogenic temperatures are presented for steel plates and weldments. These data further demonstrate the suitability of this steel for cryogenic service and provide the designer with information that should enable development of safe and economical containment systems.

Introduction

One of the most promising short term solutions for the worldwide increase in energy demand is the importation of liquid natural gas (LNG). This has already begun in several locations, and many more projects are planned to ship LNG from the rich producing countries into energy deficient markets around the world (Ref. 1). In addition, a considerable number of onshore gas processing facilities must be built. These will substantially increase the need for cryogenic containment materials capable of service at temperatures down to −260 F. Interest also remains strong for more economical materials for the containment of oxygen at −297 F and nitrogen at −320 F.

Nickel steels have been successfully used for many years for handling these liquefied industrial gases, and are prime candidates for the tank material in large ocean going LNG ships and onshore gas processing facilities. Recognizing the growing need for a more economical material for low temperature service, Armco introduced a 5% nickel alloy steel* specifically designed for cryogenic service.

This steel offers about a 20% cost savings over 9% nickel steel and has equivalent strength and toughness at −260 F. Five percent nickel steels are not really new for low temperture service because they have been used in Europe to a limited extent for some time. Some European countries have for several years included a normalized 5% nickel steel in their specifications for ethylene containment at −155 F. Now, however, the use of 5% nickel steel has been extended down to even lower service temperatures by optimization of the composition and control of the microstructure through a unique heat treatment.

This steel has been adopted by the American Society for Testing Materials (ASTM) as A645, has been incorporated in Sections II and VIII, Divisions 1 and 2 of the American Society of Mechanical Engineers (ASME) Boiler and Pressure Vessel Code as SA-645, and has been included in the American Petroleum Institute (API) Standard 620 Appendix Q for low pressurized ethylene and LNG storage tanks. To gain these code and specification approvals, the metallurgical properties of the steel have been well documented. Many weld procedure qualification tests were made by Armco and interested fabricators. These included all welding processes and filler metals currently used in welding 9% nickel steel. The data demonstrated that weldments made of this 5% nickel steel were suitable for cryogenic service, provided reasonable welding heat inputs were used.

For the past year, fatigue and fracture toughness tests have been conducted on base plate and weldments. Results of this work are reported in this paper.

Material Characterization

Description

The steel is essentially a low carbon, 5% nickel steel with about ¼% Mo added. Mn and Si are normal for alloy steels, but P and S are kept at low levels to insure maximum notch toughness. The ASTM A645 specification requires 65 ksi minimum yield strength and 95/115 ksi tensile strength. Minimum average

D. A. SARNO is Senior Research Metallurgist and J. P. BRUNER is Manager, High Carbon and Alloy Steel Research, Armco Steel Corporation, Middletown, Ohio. G. E. KAMPSCHAEFER is Manager, Technical Services at Armco's Houston, Texas plant.

Cryonic 5 produced by Armco Steel Corporation.

Charpy V-notch (2 mm deep) toughness requirements at −275 F are 25 ft-lb longitudinal, 20 ft-lb transverse, and 15 mils lateral expansion. For pressure vessel applications below −275 F, Section VIII of the ASME Boiler Code requires that no-break performance, as measured by the Drop Weight Test (ASTM E-208) be demonstrated.

The key feature of CRYONIC 5 is a new three-step heat treatment that produces the excellent combination of properties. This treatment involves conventional quenching, temperizing, and reversion annealing. These latter two treatments involve heating to specific temperature ranges in the two phase (alpha + gamma) region and cooling therefrom at specific rates. The microstructure is refined by controlling the amount of stable austenite, ferrite and low carbon tempered martensite. This structure accounts for the combination of high strength, ductility, and exceptional notch toughness. A complete description of the heat treatment and its detailed effect on microstructure has been reported previously (Ref. 2).

Base Metal Properties

Production processed ¼, ⅝, and 1½ in. thick plates from an air melted 100 ton heat of the 5% nickel steel were used in the present study. Chemical analysis, tensile properties, and notch toughness properties are listed in Tables 1 and 2. Room temperature yield strengths ranged from about 90 ksi in ¼ in. thick plates to about 67 ksi in the 1½ in. thick plate. Corresponding tensile strengths ranged from about 103 ksi in. thick plates to about 98 ksi in the 1½ in. thick plate. Cryogenic tensile tests on the 1½ in. thick plate showed yield and tensile strengths, as high as 104 ksi and 165 ksi at −320 F without a significant loss in ductility. The base plate modulus of elasticity (E) increased from 28.7 × 10^6 psi at ambient temperature to 30.7 × 10^6 psi at −320 F.

Minimum transverse Charpy V-notch lateral expansions at −320 F for the ¼, ⅝, and 1½ in. thick plates were 46, 46, and 27 mils, respectively. Nil Ductility Transition (NDT) temper-

Table 1 — Composition and Mechanical Properties of CRYONIC 5 Steel

	Chemical composition								
	C	Mn	P	S	Si	Ni	Mo	Al	N
ASTM A645	.13 max.	.30/ .60	.025 max.	.025 max.	.20/ .35	4.75/ 5.25	.20/ .35	.05/ .12	.02 max.
Heat Analysis	.08	.60	.010	.009	.25	5.03	.30	.08	.010

Plate thick., in.	Test temp., F	Spec. location	Tensile Properties Y.S., ksi	T.S., ksi	Elong. %	Red. area, %	Mod. of elast'y E × 10^{-6}, psi
ASTM A645 Req'ments			65 min.	95/115	20	——	————
¼	+75	L	88.6	104.3	32	——	————
		T	90.5	105.6	34	——	————
¼	+75	L	89.3	99.5	34	——	————
		T	92.2	100.9	37	——	————
⅝	+75	L	87.6	103.1	30	77	————
		T	84.4	101.8	30	72	————
1½	+75	L	67.9	99.6	32	72	28.74
		T	67.4	98.2	34	74	————
	-100	L	63.0	122.4	30	70	————
	-200	L	75.6	135.0	28	68	————
	-320	L	104.4	164.8	29	62	30.73

Table 2 — Charpy V-Notch Impact Properties of Cryonic 5 Steel

Plate thick., in.	Test temp., F	Spec. location	Absorbed energy, ft-lb Indiv.	Avg.	Min.	Lateral expansion, mils Indiv.	Avg.	Min.
Requ'd	−275	L	———	25	20	———	15	15
		T	———	20	16	———	15	15
1/4[(a)]	−270	L	56,55	56	55	72,64	68	64
		T	48,53	50	48	59,61	60	59
	−320	L	50,53,54	52	50	74,68,70	71	68
		T	44,46,47	46	44	66,57,63	62	57
1/4[(a)]	−270	L	43,45,43	44	43	60,60,62	61	60
		T	33,34,32	33	32	44,51,50	48	44
	−320	L	41,42,42	42	41	60,62,61	61	60
		T	30,31,30	30	30	46,46,46	46	46
5/8[(b)]	−270	L	98,[(c)]	>98	98	56,[(c)]	>56	56
		T	92,76	89	76	55,47	51	47
	−320	L	84,89,87	90	84	60,63,67	63	60
		T	56,59,60	58	56	46,47,48	47	46
1-1/2[(b)]	−270	L	84,85,88	86	84	57,58,63	59	57
		T	82,90,97	90	82	56,64.65	62	56
	−320	L	57,59,60	59	57	42,43,44	43	42
		T	36,40,44	40	36	27,30,30	29	27

(a) Half Size Specimens 10 mm × 5 mm
(b) Full Size Specimens 10 mm × 10 mm
(c) Specimens did not break when tested on 120 ft-lb capacity machine

ature tests (ASTM E-208) on the ⅝ and 1½ in. thick plates showed "no break" performance at −320 F. This establishes the NDT temperature below −320 F. Composition and mechanical properties of the heat treated plates met requirements of ASTM A645 and the ASME Boiler and Pressure Vessel Code, as shown in the tables.

Weldment Properties

Five weldments were prepared using two of the more popular welding processes presently used for joining cryogenic nickel alloy steels. These processes were pulsed-power gas metal-arc welding (PP-GMAW) and shielded metal-arc welding (SMAW). Table 3 lists the details for each welding procedure. One PP-GMAW weldment was prepared in each of the three plate thicknesses with Inconel 92 (AWS Classification ERNiCrFe-6 of AWS A5.11) filler metal in the vertical position. A fourth PP-GMAW weldment was prepared with ¼ in. thick plate in the flat position. One vertical SMAW weldment was made with Inco-Weld B electrodes in ¼ in. plate. In each case, the weld length was oriented parallel to the plate rolling direction so that transverse heat-affected zone (HAZ) impact tests could be made.

Weldments were tested in accordance with Sections VIII and IX of the ASME Boiler and Pressure Vessel Code that require tensile, bend, and Charpy V-notch impact tests of the heat-affected zone. Notch placement for Charpy specimens from each weld joint was made in accordance with the Marine Engineering Requirements (Ref. 3) of the U.S. Coast Guard and the American Bureau of Shipping Rules (Ref. 4) for low temperature cargo tanks. Notch tip placements were in the center of the weld metal, at the fusion line, and in the heat-affected zone at 1, 3, and 5 mm distances from the fusion line. Charpy V-notch impact tests were conducted at −270 F, as specified in the Marine Engineering Requirements for LNG service.

Mechanical properties of each weldment are listed in Tables 4 and 5. All weldments exhibited room temperature tensile strengths of at least 99 ksi. Tensile specimens fractured either in the base metal or the weld metal. All bend tests were satisfactory. Modulus of elasticity determinations on all-weld-metal (Inconel 92) specimens showed an increase from 26.9×10^6 psi at ambient temperature to 29.4×10^6 psi at −320 F. This 9% increase compares with a 7% increase in the base plate. Minimum average −270 F HAZ Charpy V-notch lateral expansions in the PP-GMAW welds were 26 and 30 mils for the ¼ in. vertical and flat weldments, and 38 and 25 mils for the ⅝ in. and 1½ in. vertical weldments. Minimum average lateral expansion in the ¼ in. SMAW Inco-Weld B weldment was 25 mils. All weldments satisfied the 95 ksi minimum tensile strength and the 15 mil lateral expansion requirements.

Fatigue and Fracture Test Methods

Fatigue Strength

Rotating beam fatigue tests were conducted on notched specimens of both base metal and deposited weld metals at −320 F. A notch stress concentration factor (K_t) of 2.7 was used on all specimens. Specimens were tested to a maximum of 100 million cycles, with the center section im-

Table 3 — Weld Qualification Procedures for Cryonic 5 Steel

	Pulsed power gas-metal arc (GMA) weldments prepared with Inconel 92(1) filler metal				SMA weldments, Inco-Weld B filler metal
Weldment	A	B	C	D	E
Thickness, in.	1/4	1/4	5/8	1-1/2	1/4
Weld position	Vert.	Flat	Vert.	Vert.	Vert.
Joint design	Single V	Single V	Single V	Double V	Single V
Included angle	70 deg	75 deg	60 deg	60/90 deg	60 deg
Shielding gas	75He-25Ar	75He-25Ar	75He-25Ar	75He-25Ar	None
Interpass temp.	100 F max.	150 F max.	100 F max.	100 F max.	150 F max.
No. of passes	3	6	6	16	3
Root opening, in.	1/8	None	1/8	None	1/8
Root face, in.	1/16	None	1/16	1/16	1/16
Electrode diam, in.	.035	.035	.045	.045	1/8 (a)
Current, dcrp A	75 to 100	110	110 to 124	105 to 125	90 (ac)
Voltage, V	19 to 25	24	19 to 24	19 to 27	26
Travel speed, ipm	3.5 to 8.8	10 to 12	3.15 to 7.26	2.9 to 7.6	3.0 to 3.5
Heat input, kJ/in.	17.1 to 27.6	13.2 to 15.8	24.6 to 41.9	26.5 to 47.2	40.1 to 46.8

(a) AWS ERNiCrFe-6

Table 4 — Qualification Tests for CRYONIC 5 Steel Weldments — Tensile and Bend Tests

Weld no.	Process	Filler metal(a)	Plate thick., in.	Max. heat input, kJ/in.	Test temp., F	T.S., ksi	Fracture loc.(b)	Bend tests(c)	Mod. of elast'y $E \times 10^6$, psi
A	GMAW	92	1/4	27.6	+75	99.5,107.3	WM,BM	2f,2r-pass	—
A	GMAW	92	1/4	15.8	+75	106.5,104.2	BM,BM	2f,2r-pass	—
C	GMAW	92	5/8	41.9	+75	101.5,99.5	BM,BM	2side-pass	—
				41.9	−100	115.7,116.0	WM,WM	—	—
				41.9	−200	123.4,124.6	WM,WM	—	—
				41.9	−320	141.9,142.1	WM,WM	—	—
D	GMAW	92	1-1/2	47.2	+75	100.8,100.8	BM,BM	2side-pass	26.87
				47.2	−100	120.8,114.3	BM,WM	—	—
				47.2	−200	134.1,128.8	WM,WM	—	—
				47.2	−320	148.6,144.3	WM,WM	—	29.35
E	SMAW	B	1/4	46.8	+75	100.4,99.1	WM,WM	2f,2r-pass	—

(a) 92 — Inconel 92, B — Inco-Weld B.
(b) WM — weld metal; BM — base metal.
(c) f — face; r — root; s — side; Mandrel Diameter = 6⅔ thickness.

mersed in liquid nitrogen contained in a styrofoam test chamber. This is the approximate number of stress cycles anticipated during the 20 year service life of an LNG tanker. All tests were conducted at a frequency of 10,000 rpm.

Fracture Toughness

The ductile behavior of CRYONIC 5 plates and weldments, as evidenced by the Charpy V-notch and NDT temperature tests, precluded the use of conventional linear elastic fracture mechanics methods. Therefore, stress intensity factors (K_c) and critical crack lengths ($2a_c$) were determined using R-curve technology. This technique is currently being explored in the USA for evaluating ductile materials.

Irwin (Ref. 5) postulated that for a given material and thickness there is a unique relationship between slow-stable crack extension and applied stress intensity factor, K. As the crack grows, the resistance to fracture increases due to increased volume of plastically deformed material just ahead of the crack. This increase can be expressed in terms of an R-curve for the material: the relationship between crack growth resistance development and crack extension. Crack growth resistance is designated K_R and has the same units as the fracture mechanics term K (ksi $\sqrt{\text{in.}}$). The intercept between a crack driving force curve, which is determined from the geometry and load distribution of a cracked component, and the crack growth resistance curve represents an equilibrium condition between crack driving force and crack growth resistance. The crack driving force increases with applied load and the crack will extend in a stable manner to a new equilibrium position. The specific crack driving force curve which becomes tangent to the R-curve determines the instability condition K_c.

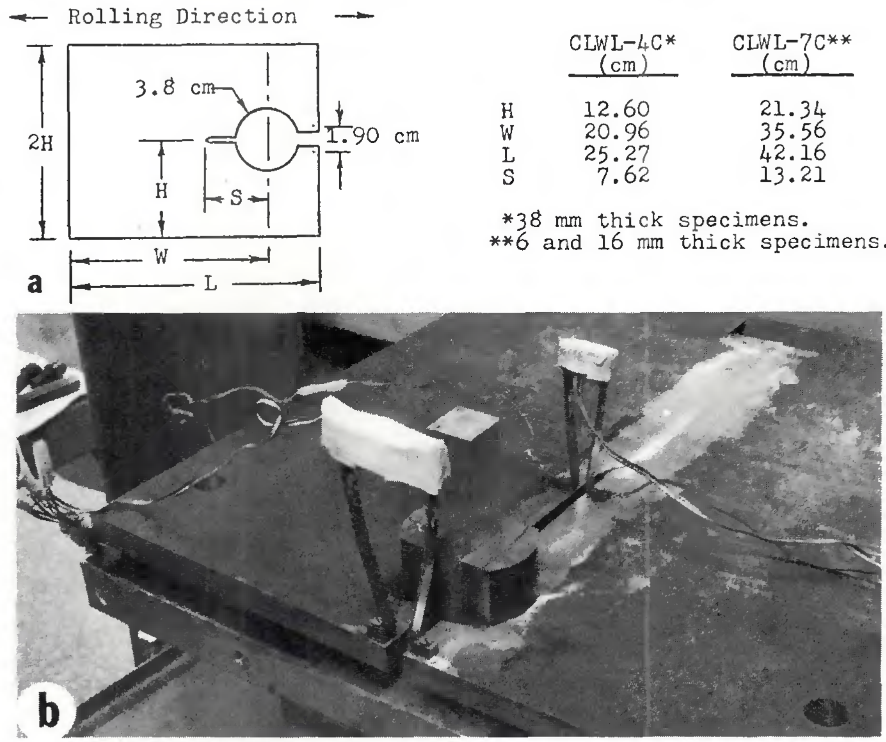

Fig. 1 — Details of the crack-line-wedge-loaded specimen. (a) Dimensions of testpiece; (b) view of the test setup showing wedge and clip gages

Table 5 — Qualification Tests for Cryonic 5 Steel Weldments: -270 F HAZ Charpy V-Notch Impact Properties[a]

Weld	Process	Filler metal[b]	Plate thick., in.	Max. heat input, kJ/in.	Notch location	Absorbed Energy, ft-lb Indiv'l	Avg.	Min.	Lateral Expan., mils Indiv'l	Avg.	Min.
A	GMAW	92	1/4[c]	27.6	WM	40,44	42	40	75,76	86	75
					F.L.	48,43,36	42	36	69,64,44	59	44
					1 mm	30,26,37	31	26	28,26,34	29	26
					3 mm	36,35,40	37	35	36,35,37	36	35
					5 mm	48,48,47	48	47	66,74,64	68	64
B	GMAW	92	1/4[c]	15.8	WM	43,38,41	41	38	61,63,62	62	61
					F.L.	35,38,35	36	35	50,61,47	53	47
					1 mm	27,38,38	34	27	28,52,36	39	28
					3 mm	28,25,38	30	25	29,26,34	30	26
					5 mm	34,34,32	33	32	40,36,46	41	36
C	GMAW	92	5/8	41.9	WM	80,83,82	82	80	50,57,63	57	50
					F.L.	88,87,96	90	87	54,50,48	51	48
					1 mm	60,101,66	76	60	31,58,38	42	38
					3 mm	(d),(d),(d)	>120	<120	(d),(d),(d)	>65	>65
					5 mm	113,(d),(d)	>113	113	64,(d),(d)	>64	>64
D	GMAW	92	1-1/2	47.2	WM	114	114	114	65	65	65
					F.L.	119,115,78	104	78	65,53,46	55	46
					1 mm	65,105,96	89	65	34,54,45	44	34
					3 mm	48,90	69	48	25,44	34	25
					5 mm	57,60	58	57	29,34	32	29
E	SMAW	B	1/4[c]	46.8	WM	18,18,18	18	18	41,42,44	42	41
					F.L.	20,20,19	20	19	34,40,48	37	31
					1 mm	26,20,20	22	20	36,16,24	25	16
					3 mm	20,39,27	29	27	16,40,21	27	16
					5 mm	32,38,30	33	30	38,58,42	46	38

(a) All weld lengths parallel to plate rolling direction yielding transverse specimens.
(b) 92 — Inconel 92; B — Inco-Weld B.
(c) Half size impact specimens 10 mm × 5 mm.
(d) Specimen did not break when tested on 120 ft-lb capacity machine.

Table 6 — Rotating Beam Fatigue (R = −1) Properties of CRYONIC 5 Steel Base Plates and Welds

Material	Thick., in.	Test temp., F	T.S., ksi	Specimen condition	10^7 Fatigue str., ksi	10^7 Fatigue str./UTS, %	10^8 Fatigue str., ksi	10^8 Fatigue str./UTS, %
Cryonic 5	3/4	+75	102.7	Smooth	58.5	57	57.5	56
				Notched[a]	27.0	26	25.0	25
	5/8	−275	140.4	Smooth	88.0	63		
				Notched[a]	35.0	25		
	1/4	−320	158.2	Notched[b]	33.0	21	29	18
Inconel 92	1/4	−320	128.4	Notched[b]	37	28	35	27
Inco-Weld B	1/4	−320	133.3	Notched[b]	37	28	35	27

(a) Stress concentration factor K = 2.5, Reference 11.
(b) Stress concentration factor K = 2.7.

Table 7 — Stress Intensity (K_C) Factors and Critical Crack ($2a_c$) Lengths for CRYONIC 5 Steel Base Plate and Weldments at −275 F

	Predicted instability conditions			
Material	Plate thick., in.	Spec. location	K ksi$\sqrt{\text{in.}}$	$2a_c$ calculated, in.[(a), (b), (c)]
Base Metal	1/4	T	355,405	140
	5/8	T	300,307	115
	1-1/4[(d)]	T	205,205	45
	1-1/2	T	207,171,205	30
Inconel 92-WM	1/4	—	375,375	160
Weldm. A-HAZ-27.6 KJI	1/4	T	440,465	220
Weldm. B-HAZ-15.8 KJI	1/4	T	475,475	255
Weldm. C-HAZ-41.9 KJI	5/8	T	410	190
Weldm. D-HAZ-47.2 KJI	1-1/2	T	196	40
Inco-Weld B-WM	1/4	—	414,414	190
Weldm. E-HAZ-46.8 KJI	1/4	T	325,325	120

(a) Based on minimum K_c value obtained.
(b) $2a_c = (2/\pi)(K_c/\delta)^2$
(c) Based on maximum allowable design stress of 23.7 ksi per ASME.
(d) Previously reported Ref. 15.

Sample calculation

1. Define 2nd order polynomial for R curve. $R = a+bx+cx^2$ where $x = \Delta a$.
2. Given $K = R$ and $dK/dx = dR/dx$ at tangency of R curve and crack driving force curve.
3. Given infinitely wide plate criterion $K = \sigma\sqrt{\pi a} = \sigma\sqrt{\pi(a_0 + x)}$.
4. Solution $\delta K/\delta x = (1/2)\sigma\sqrt{\pi}(a_0 + x)^{-1/2}$
   $(a_0 + x)^{1/2} = K/\sigma\sqrt{\pi}$
   $\delta K/\delta x = (1/2)\sigma^2\pi/K = \delta R/\delta x$; since $K = R$, $(1/2)\sigma^2\pi/R = \delta R/\delta x$
   $R = (\sigma^2\pi/2)(\delta R/\delta x)^{-1}$ and solve for x.

A crack-line-wedge-loaded (CLWL) specimen, shown in Fig. 1(a), was used to develop crack growth resistance curves (Ref. 6). The crack is driven into the specimen by a wedge and a circular segment arrangement, as shown in Figure 1(b). Clip gauges are used to measure displacement along the crack line and a double compliance technique is used to determine effective crack length. In this specimen, the crack is driven slowly until either a maximum or plateau K_R is developed or the specimen fails catastrophically. The resulting crack growth resistance curve can then be coupled with the appropriate geometrical analysis for the infinitely wide plate and an instability K_c value determined. Critical crack lengths are then calculated using assumed gross stress levels.

R curves were developed on base plates of each thickness, both deposited weld metals, and in the HAZ of all five weldments at −270 F. The test temperature was maintained within ± 5 F by electronically controlling the injection of liquid nitrogen into the cryogenic chamber.

Fatigue Crack Propagation

The most useful characterization of the fatigue crack propagation behavior of a material is a determination of crack growth rates (da/dN) as a function of the fracture mechanics stress-intensity factor range (ΔK). Paris and Erdogan (Ref. 7) showed that the functional relationship between da/dN and ΔK was best described by a single power-law curve of the form $da/dN = C\,\Delta K^n$ which results in a rectilinear plot on logarithmic coordinates. C is an experimentally determined constant and n is the slope of the power-law curve. In the most general case, the entire fatigue crack growth curve is sigmoidal when plotted on logarithmic coordinates (Refs. 8,9). The lower inflection point denotes a fatigue threshold or value of ΔK below which cracks are essentially nonpropagating. It usually occurs at crack growth rates between 10^{-8} and 10^{-9} in. per cycle (Ref. 10). The upper inflection point is where crack growth accelerates to instability. Normally only a small percentage of the total fatigue life is spent beyond this point. Most of the useful fatigue life is described by the single power-law portion of the sigmoidal curve which is bounded by the lower threshhold value and the upper instability point.

The fatigue crack growth rate as a function of the stress intensity factor range was determined for each thickness of base plate, both deposited weld metals and in the HAZ of all five weldments at −275 F. A description of the compact tension specimen, calibration test apparatus and experimental procedure used is presented by Bucci, et al (Ref. 11). The test temperature was maintained by an electronic servocontrolled solenoid valve triggered to eject liquid nitrogen coolant into a refrigeration chamber. All fatigue loading was sinusoidal zero to tension and a compliance technique for converting displacement measurements to crack length was used.

Fatigue and Fracture Results

Fatigue Strength

Rotating beam fatigue test results are presented in Table 6. For comparison, previously reported (Ref. 12) smooth and notched (K_t=2.5) base metal specimens tested at room temperature and −275 F are shown. The 100 million cycle (10^8) fatigue strength at room temperature for smooth specimens was reported to be 57.5 ksi or 56% of the room temperature tensile strength. The 10^8 notched fatigue strength at room temperature was 25 ksi or 24% of the tensile strength. The increase in tensile strength at −275 F due to the lower temperature was accompanied by a corresponding increase in fatigue performance. The smooth 10 million cycle (10^7) fatigue strength was 88 ksi at −275 F, or 63% of the tensile strength at that temperature. The notched (10^7) fatigue strength was 35 ksi or 25% of the tensile strength.

Results of the notched ($K_t = 2.7$) base metal and weld metal fatigue studies after 10^8 cycles at −320 F are shown in the table. Performance of the Inconel 92 and Inco-Weld B filler metals can be described by a single S-N curve. The 10^8 cycle fatigue strength of these notched weld metals was 35 ksi or about 27% of the tensile strength at −320 F. The 10^8 cycle fatigue strength of the notched base metal specimen was 29 ksi or 18% of the −320 F tensile strength. The finding that base metal fatigue strength is limiting for stress concentrations greater than 2.5 confirms previously reported results (Refs. 13,14). The ratio of fatigue strength to tensile strength of CRYONIC 5 under these conditions is virtually the same as results obtained on 9% nickel steel and reported elsewhere (Ref. 13).

Fracture Toughness

Stress intensity (K_c) factors and critical crack lengths ($2a_c$) for CRYONIC 5 Steel base plate and weldments at −275 F are listed in Table 7. In each case, the starting cracks were placed in the material to be evaluated, such as the HAZ or weld metal, and the crack was allowed to seek the path of least fracture resistance. Representative R-curves are schematically illustrated in Fig. 2. Smooth R-curves were obtained in all weld metal tests while many pop-in events were experienced in the base metal and HAZ tests, producing discontinuous type R-curves.

These results are comparable to those on 9% nickel steel weldments (Ref. 13). The R-curve work incorporates crack extension determinations through double compliance measurements which make it possible to follow toughness development beyond incipient crack initiation. In these materials, the toughness continues to increase after crack initiation, as shown by the rising R-curve. The multiple pop-ins indicate sufficient toughness to arrest running cracks. In view of this, K_c values at maximum K_R are reported instead of K at first pop-in as is oftentimes done with smaller test specimens of the three-point bend type.

The following analysis of the data in Table 7 is based on the lowest K_c value obtained for each replicate set of tests:

1. Base metal K_c values decreased with increasing thickness, from 355 ksi $\sqrt{in.}$ in ¼ in. plate to 171 ksi $\sqrt{in.}$ in 1½ in. plate.
2. Both weld metals had higher K_c values than any thickness of base metal tested.
3. HAZ K_c values were generally high, but varied relative to the weld metal and base metal. This variation was explained by examining the crack paths. The cracks did not always remain in the HAZ but changed directions, usually terminating in the lower strength weld metal. This change in crack direction could cause an increase in absorbed energy and result in higher K_c values.
4. Increasing the welding heat input for ¼ in. plates decreased the HAZ K_c values. As the heat input was raised from 15.8 kJ/in. in weldment B to 27.6 kJ/in. in weldment A to 46.8 kJ/in. in weldment E, the HAZ K_c values decreased from 475 ksi $\sqrt{in.}$ to 440 ksi $\sqrt{in.}$ to 325 ksi $\sqrt{in.}$ While the absolute level of K_c for all three weldments was high, this trend of decreasing toughness with increasing heat input as previously shown with conventional notch toughness tests was consistent with past experience with most heat treated steels and is especially noticeable in thinner plates.

Critical crack lengths listed in Table 7 were calculated using the lowest stress intensity factor (K_c) from duplicate tests, the maximum ASME allowable design stress of 23.7 ksi and an infinitely wide plate analysis. The calculated critical crack lengths

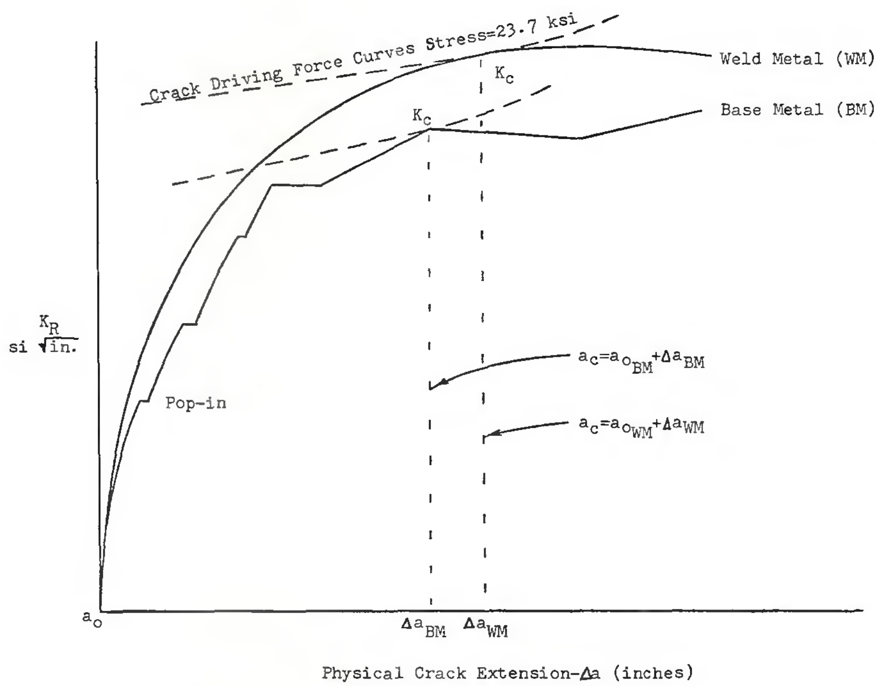

Fig. 2 — Schematic R curves illustrating crack growth resistance of weld metal and base metal

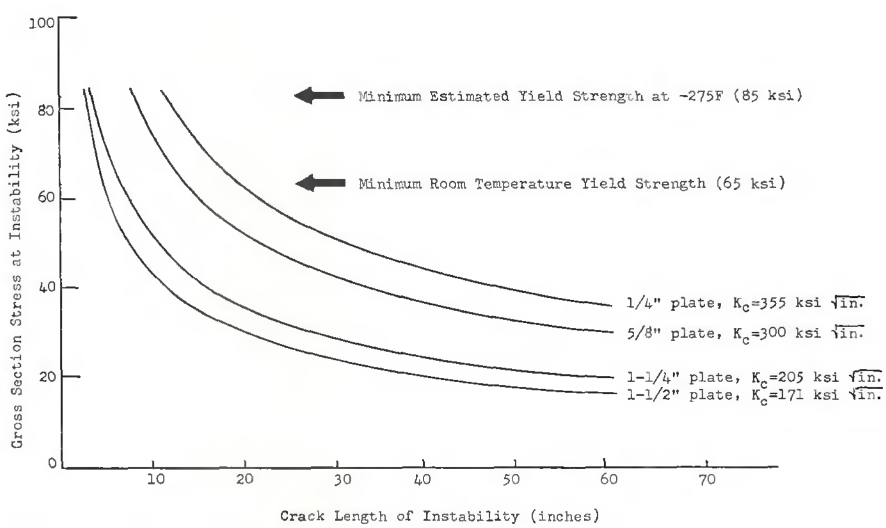

Fig. 3 — Fracture strength curves for CRYONIC 5 steel at −275 F

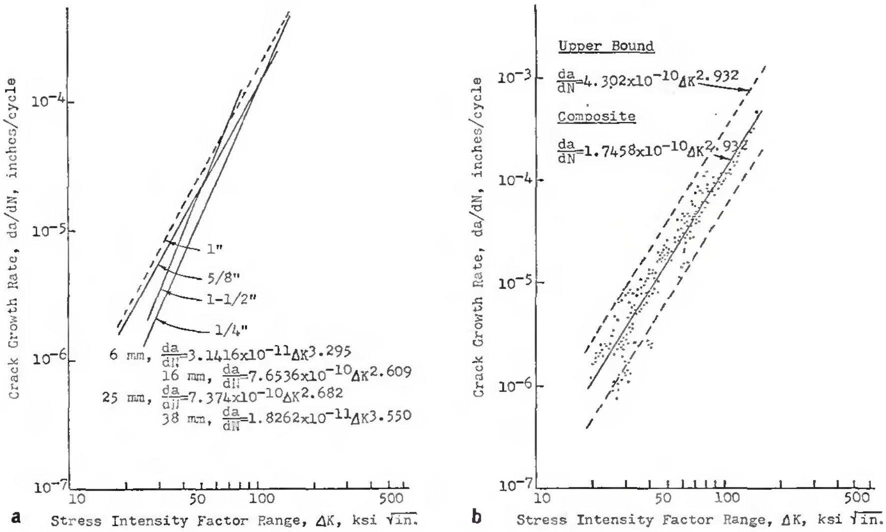

Fig. 4 — Fatigue crack growth rate for CRYONIC 5 steel base metal. (a) Individual best fit curves; (b) composite best fit curves

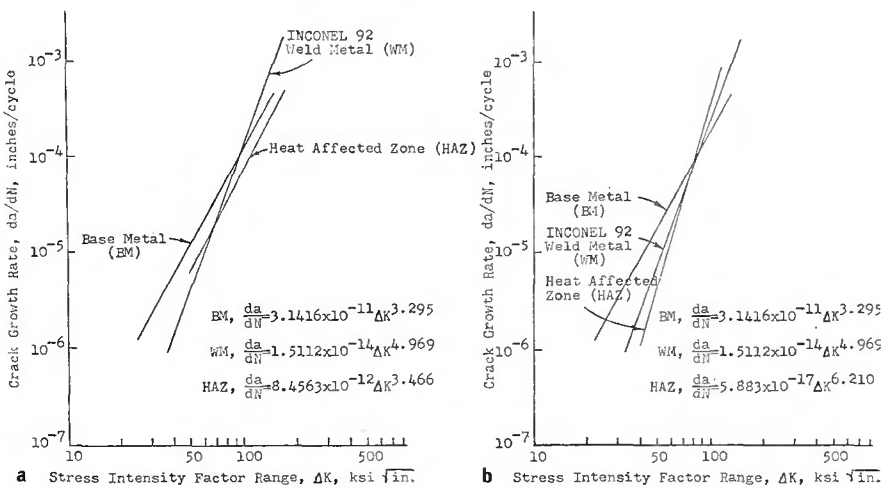

Fig. 5 — Fatigue crack growth rate of ¼ in. CRYONIC 5 GMA weldments at −275 F. (a) Weldment A, 15.8 kJ/in.; (b) weldment B, 27.6 kJ/in.

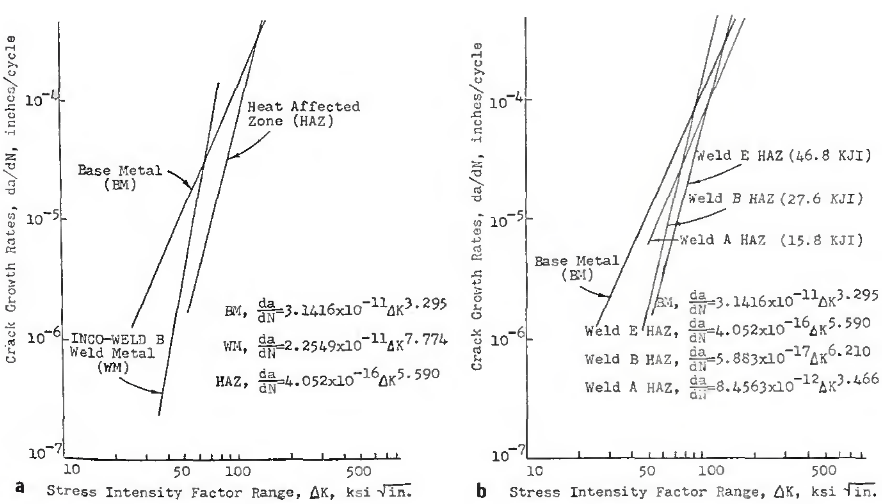

Fig. 6 — (a) Fatigue crack growth rate of ¼ in. CRYONIC 5 SMA (46.8 kJ/in.) weldment E at −275 F, and (b) the effect of increasing heat input on HAZ crack growth rates

ranged from 140 in. for ¼ in. thick base plate to 30 in. for the 1½ in. plate. Critical crack lengths for each plate thickness and stress levels up to yield strength are shown on the fracture strength curve in Fig. 3. These results imply a leak before break situation.

Fatigue Crack Propagation

Figure 4(a) summarizes the −275 F fatigue crack propagation data obtained on the ¼, ⅝ and 1½ in. thick base plates used in this investigation. Also included for comparison are crack growth rate data for the 1 in. thick plate, reported by Bucci (Ref. 11). These data indicate little effect of thickness on the fatigue crack growth rate in the ¼ to 1½ in. thickness range. The composite fatigue crack growth rate may be described by the best fit equation, as shown in Fig. 4(b).

$$da/dN = 1.7458 \times 10^{-10}\ \Delta K^{2.932}$$

for da/dN in inches/cycle
and ΔK in ksi $\sqrt{\text{in.}}$

or a more conservative approach would be to use the upper bound (2σ limit) equation, also shown,

$$da/dN = 4.302 \times 10^{-10}\ \Delta K^{2.932}$$

Fatigue crack propagation data for ¼ in. thick weldments are shown in Fig. 5 and 6. Comparison of base metal, weld metal, and heat-affected zone crack growth rates for each individual weldment (Figs. 5(a), 5(b), and 6(a)) indicate that the base plate had the fastest growth rate at ΔK values below 80 ksi $\sqrt{\text{in.}}$ for GMAW weldments and below 60 ksi $\sqrt{\text{in.}}$ for the SMAW weldment. This effect has been observed by Bucci, et al (Ref. 11) in tests with 5% nickel steel weldments and by Sarno, et al (Ref. 13) in tests on 9% nickel steel weldments. It has been attributed to residual stresses in the weldments which exert closure forces on the fatigue crack tip and hence diminish the actual ΔK that the weld metal or HAZ experiences. Data in Fig. 6(b) compare the crack growth rates of the base metal to those in the HAZ of each ¼ in. weldment. For ΔK values less than 60 ksi $\sqrt{\text{in.}}$ there was a slight increase in HAZ crack growth rate as the welding heat input was increased.

Figures 7(a) and 7(b) summarize the crack growth data obtained on the ⅝ and 1½ in. thick GMAW weldments. As observed in the ¼ in. weldments, the weld metal and each heat-affected zone had a slower crack growth rate than the base metal up to some level of ΔK. In these thicker weldments that ΔK value is approximately 100 ksi $\sqrt{\text{in.}}$

All of the heat affected zone crack growth data are summarized in Fig. 8(a). These data fall within a single band indicating little effect of thickness on the crack growth rate of the heat-affected zones in the ¼ to 1½ in. thickness range. The composite HAZ crack growth rate may be described by the best fit equation as shown in Fig. 8(b).

$$da/dN = 3.1154 \times 10^{-14}\ \Delta K^{4.7269}$$

for da/dN in inches/cycle and ΔK in ksi $\sqrt{\text{in.}}$

or by the more conservative upper bound (2σ limit) equation:

$$da/dN = 8.198 \times 10^{-14}\ \Delta K^{4.7269}$$

Fatigue crack growth data can be coupled with the fracture toughness data to estimate the useful life in terms of the total number of cycles to leak or to fracture for any cryogenic containment system when the actual load spectrum is available.

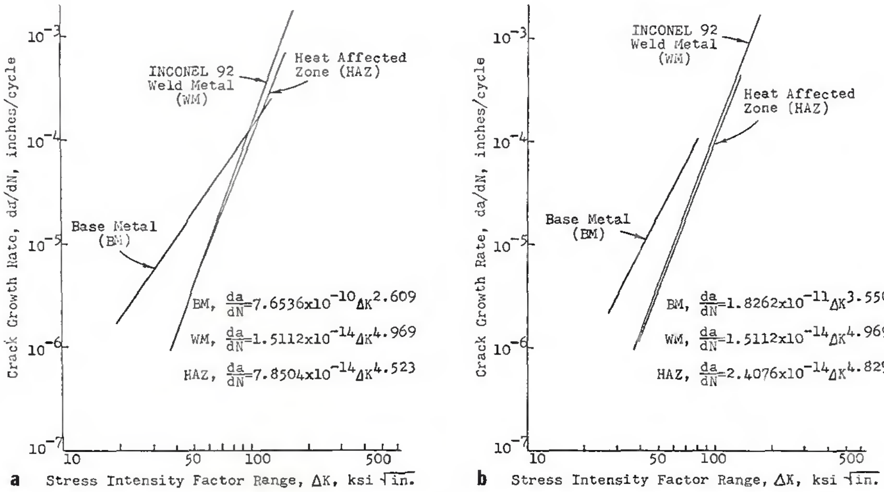

Fig. 7 — Fatigue crack growth rates of ⅝ and 1½ in. CRYONIC 5 GMA weldments at −275 F. (a) ⅝ in. weldment C; (b) 1½ in. weldment D

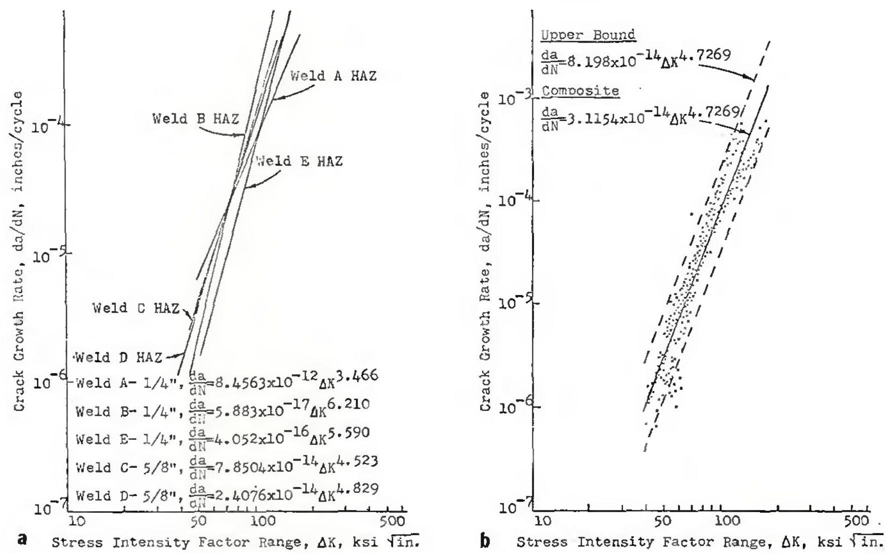

Fig. 8 — Fatigue crack growth rates of Cryonic 5 steel heat-affected zones at −275 F. (a) Individual best fit curves; (b) composite best fit curve

Summary

The suitability of welded CRYONIC 5 steel for use in cryogenic containment systems has been further demonstrated. Rotating beam fatigue, stress intensity (K_c), and fatigue crack growth rate tests were conducted on ¼ to 1½ in. thick weldments prepared with Inconel 92 (GMAW) and Inco-Weld B (SMAW) filler metals.

All strength, bend, and impact requirements of the ASME Boiler and Pressure Vessel Code and the U.S. Coast Guard were met.

Rotating beam fatigue tests showed that the notched (K_t = 2.7) 100 million cycle fatigue strength of the base metal was about 29 ksi at −320 F compared to 35 ksi for welds deposited with both filler metals.

Stress intensity factors (K_c) and critical crack lengths ($2a_c$) were determined for base plate, heat-affected zones (HAZ) and weld filler metals at −275 F using R-curve technology. Highest K_c values were obtained in weld filler metals. Base metal K_c values varied from 355 ksi $\sqrt{\text{in.}}$ in ¼ in. thick plate to 171 ksi $\sqrt{\text{in.}}$ in 1½ in. thick plate. Increasing the weld heat input in ¼ in. thick weldments from 15 to 45 kJ/in. decreased the HAZ K_c values from 475 ksi $\sqrt{\text{in.}}$ to 325 ksi $\sqrt{\text{in.}}$ The minimum critical crack length, calculated using the lowest K_c value, the present ASME Boiler Code allowable design stress, and an infinitely wide plate analysis, was 30 in. for the 1½ in. thick base metal.

Fatigue crack growth rate (da/dN) as a function of the stress intensity factor range (ΔK) was determined on through-cracked compact tension specimens for each thickness of base plate, weld metal deposited by two filler metals and in the HAZ of five weldments at −275 F. Highest growth rates occurred in the base metal. There was little effect of thickness on growth rates of either base plate or HAZ in the ¼ to 1½ in. thickness range. General fatigue crack growth rates were determined, and from this information useful life in terms of total number of cycles to leak or fracture for any cryogenic containment system may be estimated.

Acknowledgments

The authors would like to thank Messrs. D. E. McCabe, T. G. Heberling, and G. C. Schmid for their contributions to this paper.

References

1. Hunsaker, B., "Natural Gas From Abroad", Seventy-First National Meeting of Am. Inst. of Chem. Engs., Dallas, Feb. 20-23, (1972).

2. Sarno, D. A., et al, "Transformations Involved in Developing Notch Toughness in a New 5% Nickel Steel for Cryogenic Applications", ASM Matls, Eng. Congress, Cleveland (1970), ASM Tech. Report No. C70-39.2.

3. Federal Register, Volume 33, Number 245, Part II, Department of Transportation — Coast Guard — Marine Engineering Requirements, December 18, 1968.

4. 1973 Rules for Building and Classing Steel Vessels, Section 24, Para. 24.65.3, ABS, New York, New York.

5. Irwin, G. R. and Kies, J. A., "Critical Energy Rate Analysis of Fracture Strength," *Welding Journal*, Vol. 33 (4) Apr. 1954, Res. Suppl., pp. 193-s to 198-s.

6. McCabe, D. E. and Heyer, R. H., "R-Curve Determination Using a Crack-Line-Wedge-Loaded (CLWL) Specimen", Frac-

ture Toughness Evaluation by R-Curve Methods, ASTM STP 527, American Society For Testing and Materials, 1973, pp. 17-35.

7. Paris, P. C. and Erdogan, F., "A Critical Analysis of Crack Propagation Laws", *Journal of Basic Engineering*, ASME Transactions, Vol. 58, Series D, No. 4, 1963, p. 528.

8. Paris, P. C. and Wei, R. P., "Fracture Mechanics in Fatigue", ASM Symposium on Engineering Aspects of Fatigue, 1969 Materials Engineering Congress, Philadelphia, Pennsylvania, 13-16 October 1969.

9. Johnson, R. E., "Some Observations of Cyclic Crack Propagation from a Fracture Mechanics Viewpoint", ASM Symposium on Metallurgical Aspects of Fatigue Fracture, Materials Engineering Congress, Philadelphia, Pennsylvania, 13-16 October 1969.

10. Paris, P. C., et al, "Extensive Study of Low Fatigue Crack Growth Rates in A533 and A508 Steels", ASTM STP 513, American Society for Testing and Materials.

11. Bucci, R. J.; Greene, B. N.; and Paris, P. C.; "Fatigue Crack Propagation and Fracture Toughness of 5 Nickel and 9 Nickel Steels at Cryogenic Temperatures", Sixth National Symposium of Fracture Mechanics, ASTM, Philadelphia, Pa., 8/28/72.

12. Metallurgical Properties of Armco CRYONIC 5 Steel, Armco Steel Publication, September 15, 1971.

13. Sarno, D. A.; McCabe, D. E.; and Heberling, T. G.; "Fatigue and Fracture Toughness Properties of 9% Nickel Steel at LNG Temperatures", presented at the ASME Petroleum Engineering Conference in Los Angeles, California, September 16-20, 1973.

14. Kunihiro, T., et al, "Low Temperature Fatigue Behavior of 9% Nickel Steel Weld Joints", International Institute of Welding, Commission XIII — Fatigue Testing, Toronto, 1972.